

Parametric Study of Temperature Effects on Traffic-Induced Response for Bridge Structural Health Monitoring

Artem Marchenko

Faculty of Engineering Technology (ET), Civil Engineering and Management (MSc), University of Twente, Enschede, Netherlands

ABSTRACT

Bridge response to varying distributed temperatures is unique. Temperature is causing major deformations in bridges that are larger than or equal to the peak-to-peak traffic loads. The correct characterization of the bridge thermal response is important to assess its performance and detect an onset of damage. The aim of this research is to characterize bridge thermal and traffic-induced responses such as vertical displacements to assess bridge conditions (e.g., damage detection). In this study, the numerical replicas (in form of a finite element model) of the UT Campus bridge, which is a steel girder bridge, are generated. Firstly, various temperature distribution scenarios such as those resulting from extreme weather conditions due to climate change are modelled. Then nominal traffic load scenarios are included, and bridge response is characterized. Finally, the damage is modelled as a reduction of material stiffness due to corrosion. The relationship between distributed temperature loads and bridge response could help with interpreting changes in it along the length of the structure, factoring in nominal traffic loads and damage. This study emphasizes the importance of accounting for distributed temperature loads in bridge response, which is important for bridge engineers to consider both in bridge design and condition assessment.

1. Introduction

Bridges are essential for civil infrastructure, allowing traffic to cross difficult terrains and obstacles. Their proper functioning is critical for the local economy and the well-being of society (Kromanis, Kripakaran, & Harvey, 2015). Therefore, effective structural management strategies are necessary. Although, they are not always achieved with costly and time-consuming visual inspections, which are performed too late when major interventions for deteriorated bridge components are needed (Brownjohn, 2007).

1.1 Structural Health Monitoring

Structural Health Monitoring detects and characterizes structural damage in critical civil infrastructure like bridges, tunnels, or wind turbines. Sensors are installed to collect data, which is analyzed to assess structural safety, strength, integrity, and performance (The Constructor, 2021). Damage can alter stiffness, mass, or energy dissipation properties, affecting the measured dynamic response of the structure (Sohn, 2006).

Data-based and model-based approaches exist. The data-based approach uses supervised and unsupervised machine learning algorithms to detect damage by extracting damage-sensitive features from the structural response. The model-based approach uses finite element modelling to identify damage by measuring structural response with a reference model and calibrating stiffness properties and boundary conditions based on recorded response. However, environmental variations such as distributed temperature and solar exposure can cause substantial uncertainties and errors in the structural response (Bud, Moldovan, Radu, Nedelcu, & Figueiredo, 2022).

1.2 Bridge Response

In practice, monitored dynamic or static responses are affected by changing environmental and operational conditions. The environmental conditions are wind, temperature, and humidity. The operational conditions are ambient, mass loadings, and operational speed (Sohn, 2006).

Temperature variations may induce stress that is ten times larger than traffic, impacting the structural health of the bridge and its components (Catbas, Susoy, & Frangopol, 2008). Bearings in bridge design compensate for both contraction and expansion caused by temperature changes, allowing for rotation and translation. When the movement is restrained, structural elements may experience excess stresses, affecting the overall performance (Goulet, Kripakaran, & Smith, 2015).

Several studies have investigated the impact of temperature variations on dynamic response. Temperature variations can alter the material stiffness and potentially change the boundary conditions of a system. Ideally, the magnitude of natural frequency is proportional to the stiffness, so when the damage increases, the frequency decreases (Farrar, et al., 1996). Moorty & Roeder (1992) showed how the Sutton Creek Bridge in Montana, USA, is affected by daily and seasonal temperature variations. The analytical model showed a considerably large expansion of the bridge deck as the temperature increased. For the daily temperature variations, the first mode's natural frequency of the bridge can vary around 5% throughout a 24-hr period (Doebbling & Farrar, 1997). For the seasonal temperature variations, the natural frequencies of the bridge can vary around 10% per year for a tested 3-year period (Askegaard & Mossing, 1998). The study on the thermal performance of the Tamar Suspension Bridge in Plymouth, UK showed that daily and seasonal temperature changes are an important consideration for the serviceability limit state of bridges. Bridge design must account for thermal expansion and contraction cycles. It is important to understand whether the structure has fixed supports and if the structural elements are able to compensate for excessive loads due to expansion or contraction (De Battista, Brownjohn, Tan, & Koo, 2015).

Mass loading from the traffic (cars, cyclists, pedestrians) is an operational variable that induces stress and is difficult to measure. Hence, data normalization is required. Kim et al. (1999) have found that measured natural frequencies of 46m long steel bridge can decrease by about 5.4% because of heavy traffic. Changes in measured natural frequencies for heavy and light traffic are hardly detectable for mid- and long-span bridges. To estimate the load-bearing capacity and investigate real structural behaviour, finite element models (FEM) are normally developed and tested. Using such models and applying static and dynamic load-tests, engineers can compare predictions with measured performance benchmarks to get an insight into making management decisions. However, epistemic uncertainties resulting from temperature changes may be present (Goulet, Kripakaran, & Smith, 2015).

Pedestrian footbridges are susceptible to both vertical and horizontal vibrations. This causes resonant responses which result in high vibration levels and the need for appropriate dynamic design. Generally, vibrations do not cause structural problems, however, they can cause discomfort to its users (i.e., pedestrians) due to exceeding acceleration values. The vertical force is more prominent than the horizontal force, however, both lateral and horizontal components can also cause vibration problems for the structure. The frequency of lateral movement is equal to half of the step of vertical and longitudinal frequency movement (Máca & Štěpánek, 2017). Deviations up to 10% in natural frequencies can occur in a detailed finite element model. The amplitude of natural frequency is influenced by the number of pedestrians. To develop a numerical model and perform the dynamic analysis, natural frequencies and vibration modes must be known (Tadeu, et al., 2022). In general, walking frequencies for pedestrian bridges are within the range of 1.6 to 2.4 Hz (Gheitasi, Ozbulut, Usmani, Alipour, & Harris, 2016).

1.3 Deflections

To ensure the structural integrity of the bridge, structural engineers are required to check for deflections and vibrations so that all values meet minimum and maximum value requirements. Deflection is a critical consideration in the serviceability problem and governs the structural design outcome. Deflection limits are used for checking whether the maximum allowable deflection limit of the structure is smaller than the measured vertical displacement value (Ji, 2020). Vertical displacement is the movement of a point or the object relative to the reference point which is used for the performance and stability assessment of the structure (Kurloo Technology Pty Ltd., 2022). Depending on the bridge type, different maximum deflection limits exist. EN 1993-1-1 Eurocode 3: “Design of steel structures” provides no guidance on the deflection limit. Therefore, in the context of this research, the international standard of span/500 deflection limit is considered (Smith, 2011).

1.4 Research Purpose

The premise of this study is to investigate the temperature effect on the traffic-induced response of a bridge in the context of SHM condition assessment. Various temperature distributions and their impact on the response are characterized under the same static load and damage conditions. The subsequent sections of this study provide a detailed description of the methodology used to model distributed temperatures and collect deflections due to static loads. The steps taken in the parametric study and the analysis results obtained during each consecutive inspection are evaluated to perform damage detection.

2. Methodology

To study temperature effects on the bridge response, multiple temperature distribution scenarios must be considered. While performing a condition assessment, it is important to collect both temperature distributions and bridge responses (e.g., vertical displacements, strains) due to static load(s). Then, compare them to each consecutive inspection when temperature distribution changes. Following the parametric approach, this study develops a methodology for determining changes in bridge response due to temperatures that are not accounted for. The finite element models (FEM) are employed because they can accurately model the structural response of the system under various loading conditions and damages (Harish, 2022).

The methodology for conducting this research is presented in a flowchart in Figure 1. The input to the methodology is temperature distribution (T) at i^{th} scenario and nominal traffic load (L) at j^{th} combination. The combination of both needs to be understood in order to characterize the bridge response, which is important for condition assessment (e.g., recognizing structural damage). Temperature distributions across the structure can directly affect its thermal response (Kromanis & Kripakaran, 2014). Therefore, bridge response during the baseline (e.g., no damage) and damage conditions must be checked for different temperature distribution scenarios to understand if changes occur. If no changes under baseline conditions can be observed, there is no need to account for temperature distributions because the bridge response stays unchanged. However, if changes in the response under damage conditions are observed, the knowledge of distributed temperature effects on the bridge's response is important.

One of the most recent condition assessment methods is the Deformation Area Difference (DAD) Method, which is presented in Figure 2. Alternatively, for long-term inspections, this method can be used for damage localization. Structural responses between baseline and damage conditions are collected, and their difference is presented as deformation area(s). Although the method has proved to work, the accuracy of its results and their precise interpretation are directly affected by the number of measurement points on the structure (Erdenebat, Waldmann, Scherbaum, & Teferle, 2018).

The DAD can be determined using Equation 1, which involves squaring the differences in the area between the deflection line curves generated by the analysed structure state and the corresponding reference system in the absence of damage. In this equation, $f_{d,i}(x)$ represents the deflection function of the damaged curve, and $f_{t,i}(x)$ represents the deflection function of the reference curve. The variable i refers to the specific area section, such as A_1 , A_2 , and so on. The term ΔA_i^2 denotes the area difference in section i , while $\sum_1^n \Delta A_i^2$ represents the total area difference of the entire structure (Erdenebat, Waldmann, Scherbaum, & Teferle, 2018).

In this study, the traffic load is taken as a UDL assumed to be applied during the bridge load test. Under baseline conditions, where only the traffic loads are applied, the response is checked for different temperature distributions. In reality, vertical deflections due to traffic load would change when new temperature distribution is present. Then, changes in the response must be observed and compared as deformation areas when temperature distributions are characterized and not characterized. If no changes are observed for traffic loading only, the new measurements must be collected for other temperature distributions. The same steps must be repeated for new measurements to detect damage. It should be noted that the obtained deflection values may be very small, although could fluctuate enough to observe and establish the pattern.

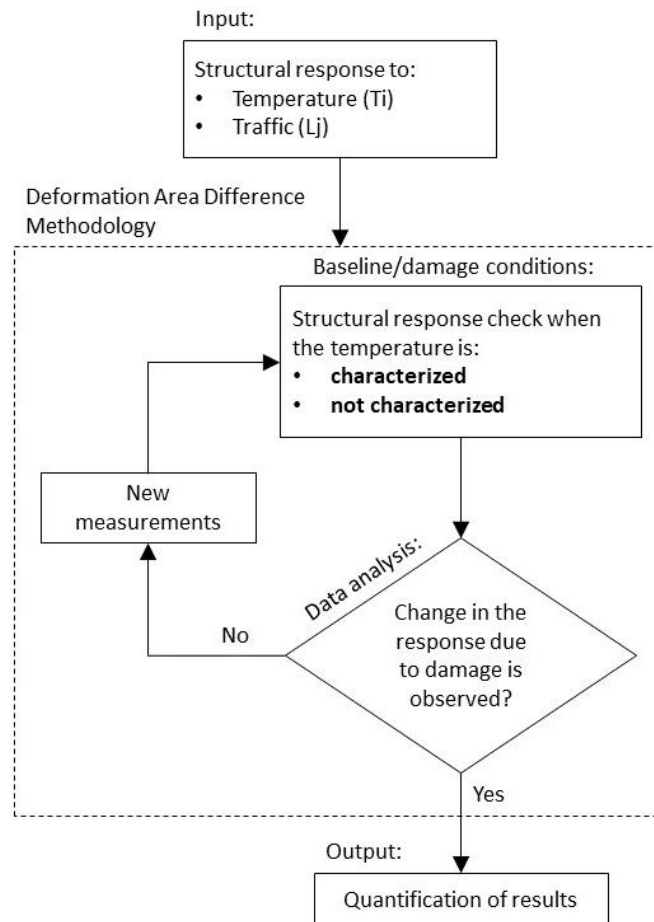


Figure 1: Methodology flowchart.

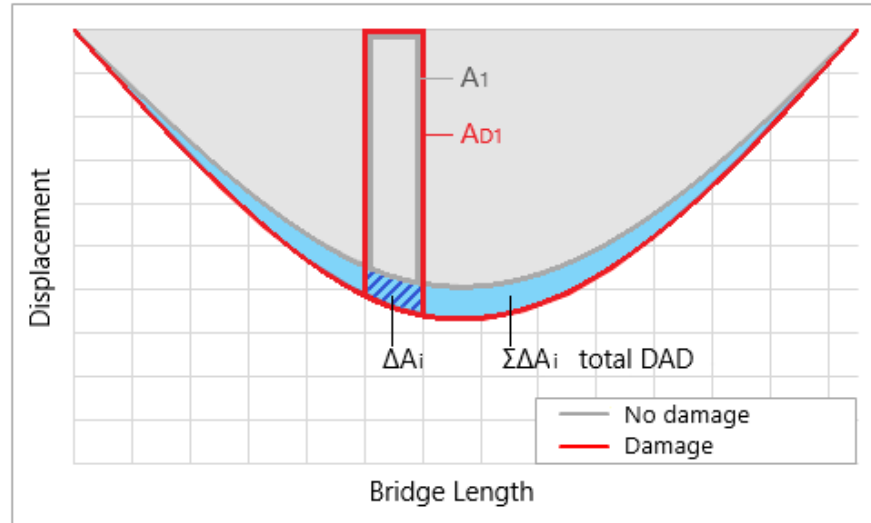


Figure 2: Example of the DAD method.

$$DAD_i(x) = \frac{\Delta A_i^2}{\sum_{i=1}^n \Delta A_i^2} = \frac{\left[\int_{i-1}^i f_{d,i}(x) dx - \int_{i-1}^i f_{t,i}(x) dx \right]^2}{\sum_{i=1}^n \left[\int_{i-1}^i f_{d,i}(x) dx - \int_{i-1}^i f_{t,i}(x) dx \right]^2} \quad \text{Equation 1.}$$

3. The UT Campus Bridge

The UT Campus bridge (Figure 3) is located at the University of Twente, the city of Enschede in the Netherlands. The bridge was possibly commenced to the public in the 1980s as a pedestrian footbridge. Spanning 27 meters long, it connects the HogeKamp (East) and the football field (West) across a pond. The bridge appears to have signs of steel corrosion. The bridge is positioned along the north-west axis. Due to a nearby tall building and trees, only the northwest side of the bridge is directly exposed to the sun during the sunrise in spring/autumn, resulting in differential thermal expansion/contraction of the structure. The north side of the bridge is mostly hidden from the sun.



Figure 3: The UT Campus bridge from the East side of HogeKamp (left) and its geolocation (right).

A structural drawing with main dimensions is shown in Figure 4. The structure of the bridge consists of three 27 meters long IPE600 steel girders and 80x80x5SHS horizontal bracings. The boundary conditions are fixed. The D40 hardwood oak timber decking and posts with handrails cover the structure. The girders of the bridge are named according to the axes on which they lay. For example, the middle girder, which is on axis B is named girder B.

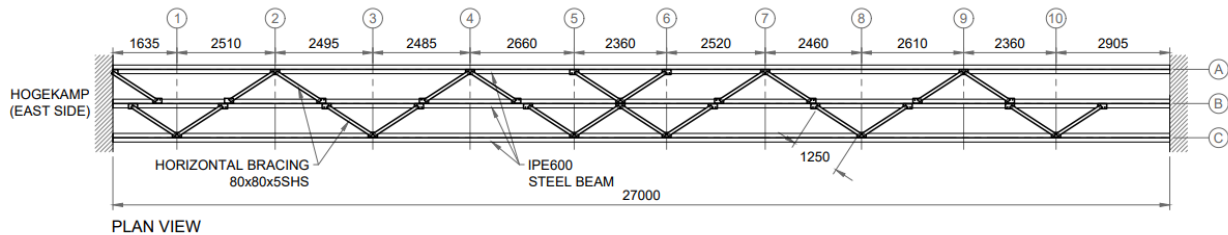


Figure 4: Structural plan view of the UT Campus bridge.

The sun's path is always changing with the season. There are two solstices, which are on the 21st of June and the 21st of December. On the June solstice, the sun's path gradually moves southward until December. At the December solstice, the sun's path gradually moves northward again, returning to the celestial equator (Schroeder, 2011). As presented in Figure 5, the longest day can be observed on (a) the June solstice, and the shortest on (b) the December solstice. Having this considered, the sun exposure is different throughout the year for this location.



Figure 5: Sun path in (a) 21 June and (b) 21 December.

The strain-temperature data collected by sensors during field measurements are presented in Figure 6. The relationship between strain-temperature on a sunny day (a) suggests that when the temperature increases, the strain tends to decrease. This can be explained by the thermal expansion of steel. However, when the temperature is constant, such as on a cloudy day (b), the strain is constant, too. The temperature is different throughout the bridge. Spikes in strain measurements can be observed due to pedestrian crossings.

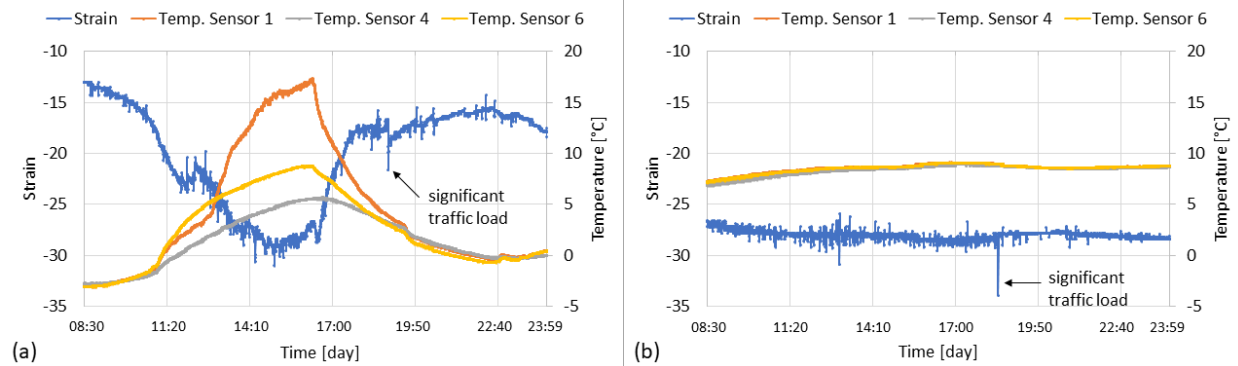


Figure 6: Strain-temperature on a sunny day (a) and a cloudy day (b).

4. Parametric Study

This section presents the parametric study of bridge response. Firstly, detailed explanations of the proposed loading and temperature distributions are discussed. Then, the reference temperature is specified. Lastly, the process of bridge modelling is elaborated, along with the calibration steps taken to validate the results of performed numerical simulations.

4.1 Modelling the Bridge

The numerical replicas of the UT Campus bridge are modelled in Ansys Mechanical APDL. Ansys is an advanced FEM software that can support static/dynamic, structural, and heat transfer analyses (Ansys, 2022). APDL, which is an acronym for “Ansys parametric design language”, is a scripting language that was used in conjunction with Ansys to numerically recreate a model (Ansys Learning, 2021).

To build the FEM (Figure 7), the MKS system of units is set, and the geometry and materials are examined. Material profiles for structural steel and D40 oak hardwood timber are created. SHELL181 is selected as an element reference system to model shell elements for the girders and decking. Using the 1/10 meshing ratio rule, the appropriate mesh is generated for the girders and decking. Horizontal bracings are connected to girders using the LINK180 element reference system. Consequently, simply supported conditions are applied and assumed for this study.

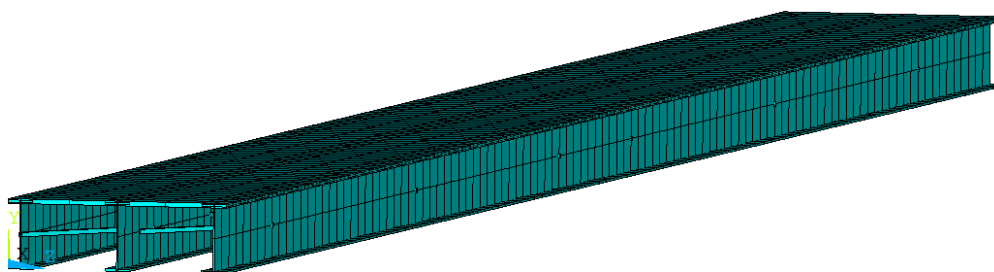


Figure 7: FEM of the UT Campus bridge.

4.2 Model Calibration

Section 5.7 “Dynamic models of pedestrian loads” of Eurocode suggests that forces generated by pedestrians with a frequency matching one of the natural frequencies of the bridge can induce resonance and must be considered in limit state verifications (European Committee for Standardization, 2003). Having this considered, multiple dynamic model simulations are performed for different boundary conditions to obtain similar natural frequencies, which ideally, help obtain true vertical displacements. Significant changes in natural frequencies are observed at different combinations of boundary conditions. The models of the two mode shapes and respective natural frequencies are shown in Figure 8. Using the simply supported conditions and restraining only the top flange of the beams at each side yielded similar modal frequencies to the observed ones. The first two frequencies of the model are 2.47 and 4.23 Hz, corresponding to the first vertical bending and torsional modes. The field measurements give around 3 and 4 Hz for the two modes, respectively.

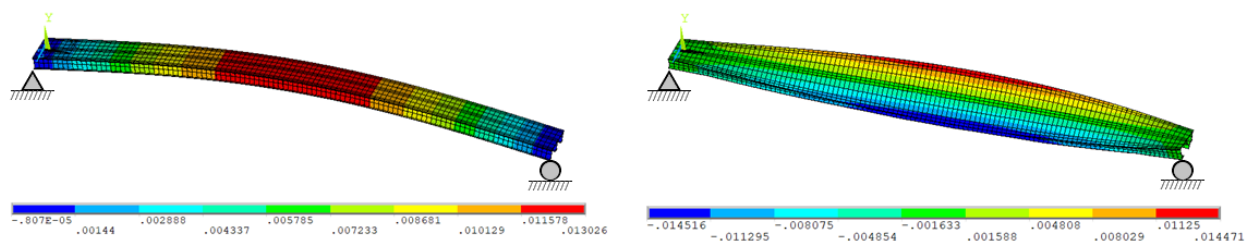


Figure 8: Dynamic behaviour: Vertical bending mode at 2.47 Hz (left) and torsional mode at 4.23 Hz (right) of the bridge.

4.3 Load-Test Scenarios

To characterize operational conditions, two pedestrian loading scenarios (Figure 9) are proposed. In the first loading scenario, L_A is a uniformly distributed load (UDL) at the centre of the mid-span of the bridge. In the second loading scenario, L_B is the same UDL applied at the side of the mid-span of the bridge. UDL is set to 4.1 [kN/m²]. This is based on the characteristic value of UDL in the serviceability limit state (Equation 2) according to Section 5.3.2.1 “Uniformly distributed load” of EN 1991-2:2003. Both loads are applied in unfavourable parts of the structure’s influence surface, where L_A would experience maximum temperature gradient and L_B ’s highest temperature in one of the scenarios, discussed in the next subsection.

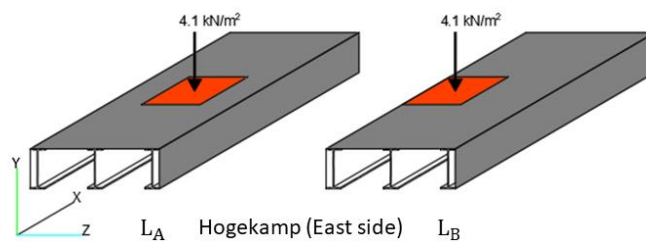


Figure 9: Loading scenarios, L_A and L_B .

$$q_{fk} = 2,0 + \frac{120}{L + 30} \text{ [kN/m}^2\text{]} \quad \text{Equation 2.}$$

Where: q_{fk} – UDL,

L – length of a load.

$$\text{Check: } 2,5 \text{ [kN/m}^2\text{]} \leq q_{fk} \leq 5,0 \text{ [kN/m}^2\text{]}$$

4.4 Temperature Distributions

Bridges experience complex temperature distributions that are typically non-linear and vary in three spatial dimensions. Depending on whether the local environment has buildings, terrain, or trees, certain parts of a bridge may or may not be fully exposed to solar radiation, hence leading to oblique temperature gradients throughout the day. Not all temperature distributions can be predicted, therefore specific and extreme temperature distributions are employed to achieve practical design (Goulet, Kripakaran, & Smith, 2015).

The UT Campus bridge has a unique position relative to the sun path and the abovementioned surroundings. Having this considered, five different temperature distributions were proposed in Figure 10. The first temperature distribution, T1 represents a cloudy winter day with an ambient temperature of 0°C. The second temperature distribution, T2 represents a hot cloudy summer day with an ambient temperature of 30°C. The T3 is a linear temperature gradient distribution along the length and depth of the structure, ranging from 8 to 20°C. This scenario recreates the sunrise in spring/autumn. The T4 is a linear temperature distribution along the width and depth of the structure, ranging from 10 to 30°C. This scenario recreates an extremely hot summer/autumn day at noon. Lastly, T5 is the same as T4 but with a temperature range from 30 to 50°C. The last scenario represents an extremely hot summer day at noon.

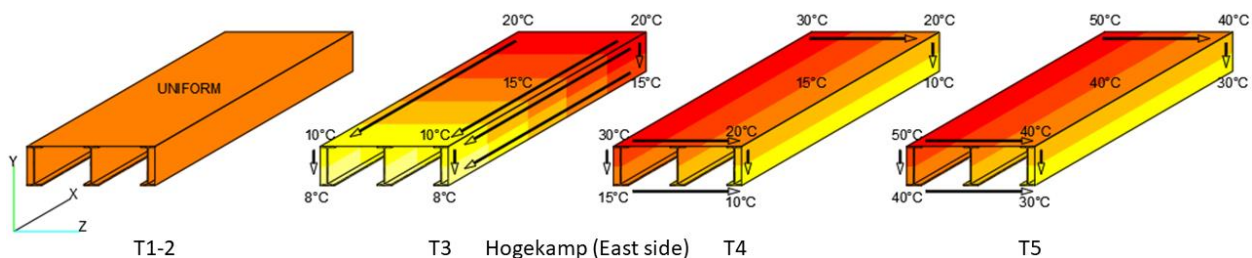


Figure 10: Temperature distributions.

The temperature distribution within the structural elements can be affected by the stored thermal energy. The surface of the structural elements can receive, emit, and reflect shortwave and longwave radiation. Depending on the environmental conditions, the surface can be cooled or heated up by evaporation, precipitation such as rain or snow, melting and freezing processes, influencing heat balance. Heat modelling is based on spatial and temporal interdependent parameters, which are used for the description of environmental conditions and material

properties and are important for simulation accuracy (Görtz, Jürgensen, Stolz, Wieprecht, & Terheiden, 2022).

The input material properties for Young's modulus, Poisson's ratio, and thermal expansion coefficients are constant. Hence, the defined material properties are specific to when the ambient temperature is 20°C.

4.5 Bridge Response

The response of the bridge girders due to two different applied UDLs is shown in Figure 11. In the first nominal traffic loading combination, L_A resulted in equal deflection for all three girders. However, L_B resulted in different vertical displacements. The deflected shape of girder A increased. Girder B remained unchanged. Lastly, the deflected shape of the girder C decreased.

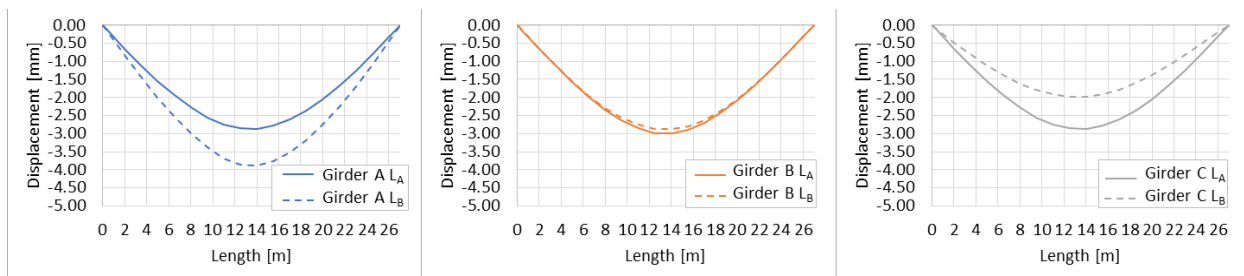


Figure 11: Traffic response for different girders.

An example of temperature load distribution on the FEM and thermal responses due to different temperature distributions are shown in Figure 12. Each temperature distribution is relative to the reference temperature of 20°C. Although the structure is at rest during the reference temperature, the negative deflection would occur if the load is applied, or the temperature increased. This implies that when a positive deflection occurs, the deflection of the bridge decreases. Furthermore, when a negative displacement occurs, the deflection increases.

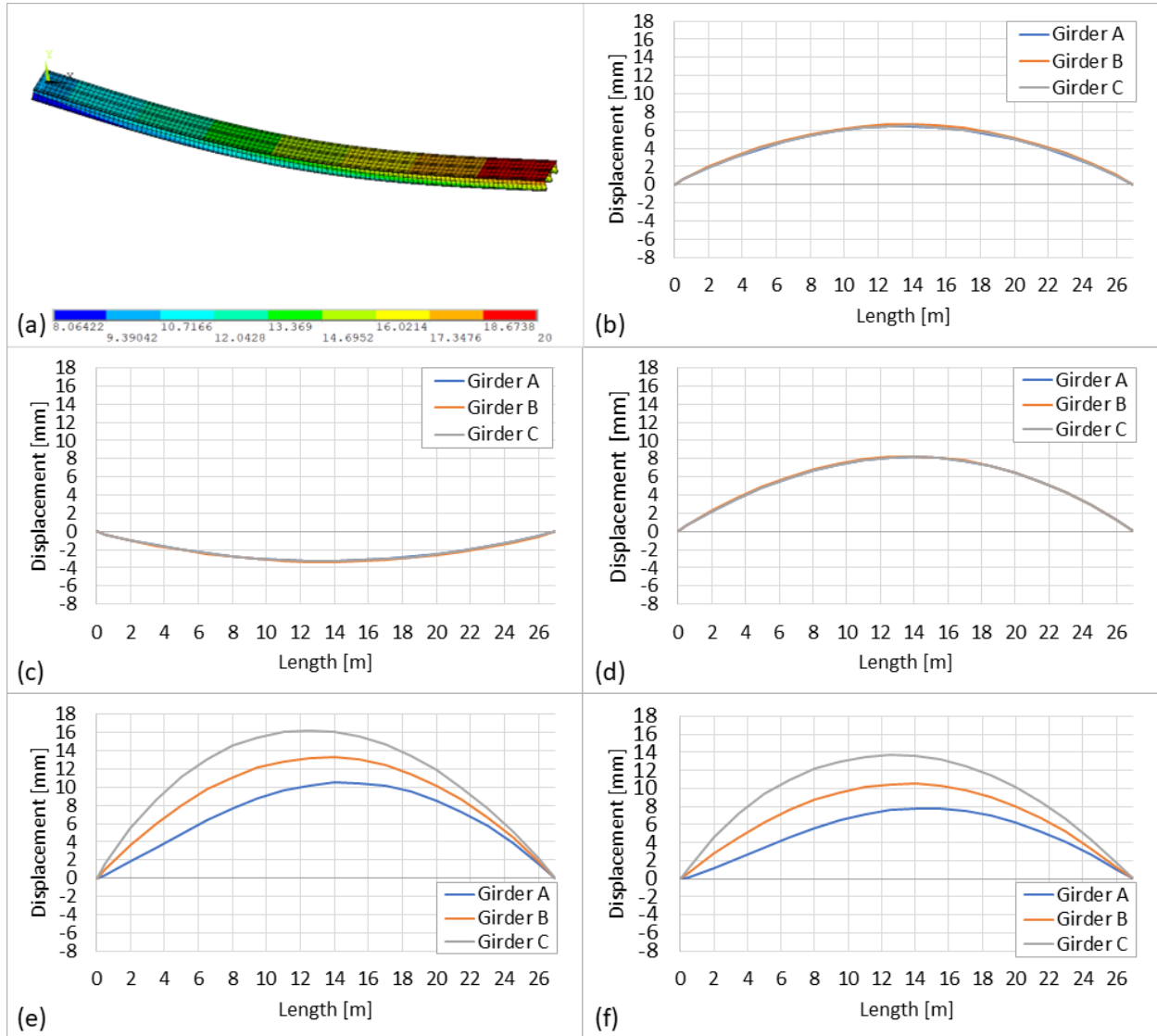


Figure 12: (a) FEM showing the deformed shape of and temperature distribution scenario T3 for the UT Campus bridge; (b) to (f) displacement of girders along the length of the bridge for scenarios T1 to T5, respectively.

In Figure 13, combinations of traffic and thermal loads are shown. Each traffic loading scenario is applied under different temperature distributions to understand if vertical displacements would deviate significantly. Overall, a similar deflection trend can be observed between two traffic loads and every temperature distribution. The discussion on vertical displacements is given in the next section.

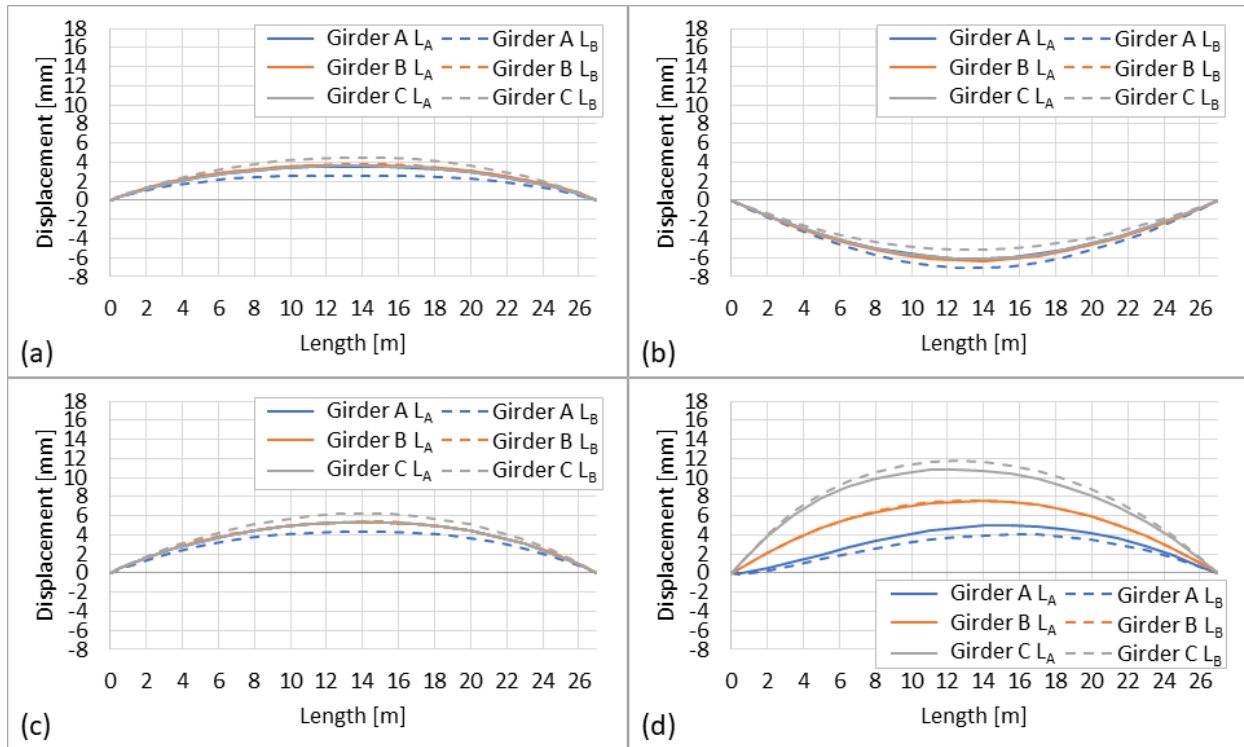


Figure 13: Traffic and thermal load responses for (a) to (c) for scenarios T1 to T3, and (d) for scenario T5, respectively.

4.6 Damage

The damage (in a form of steel corrosion) is simulated to study the response of different traffic and thermal loads. In Figure 14, the damage at the bottom flanges of girders A, B, and C is induced by decreasing Young’s modulus by 10%, 7.5%, and 5%, respectively.

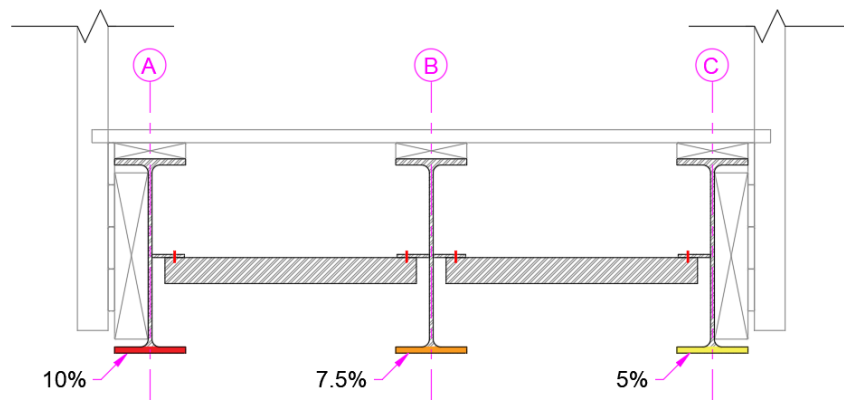


Figure 14: Damage conditions.

5. Results

5.1 Bridge Response

In Figure 11, when only traffic loading L_B is applied to the bridge at the reference temperature of 20°C , maximum vertical displacement decreases by 1 [mm] at girder A, increases by 0.11 [mm] at girder B and 0.89 [mm] at girder C. Opposite vertical displacements can be observed at girders A and C. The change at girder B is insignificant.

In Figure 12, at T1, when the temperature is 0°C , all girders experience positive symmetrical deflection of 6.5 [mm] at the mid-span. At lower temperatures, thermal contraction occurs leading to an increase in the ultimate tensile strength (Levings & Sritharan, 2012). Therefore, the deflection would decrease. At T2, when the temperature is 30°C , all girders experience a negative symmetrical deflection of 3.25 [mm] at the mid-span. Although temperature changes are rarely uniform, the uniform increase in temperature on the simply supported girder can cause elongation and result in the development of excess stresses (Brenner, et al.). Therefore, the deflection would increase. At T3, linear temperature distribution along the length and depth of the structure ranges from 8 to 20°C . This leads to a large positive symmetrical deflection of 8.2 [mm] at the mid-span. In the last two temperature distributions along the width and depth, positive unsymmetrical deflections can be observed at the mid-span. At T4, vertical displacements for girders A, B, and C are 10.5, 13.3, and 16.2 [mm], respectively. At T5, vertical displacements for girders A, B, and C are 7.8, 10.5, and 13.7 [mm] respectively. Girder A experiences the smallest vertical displacements due to extreme temperature distribution, while girder C has the largest due to lower temperature.

5.2 Damage

When the damage is present, the bridge response for each nominal traffic loading combination is slightly different (Figure 15). At the reference temperature of 20°C , maximum vertical displacement in girders increases by 3-4%. Due to slightly higher damage at girder A, moderate at girder B, and smallest at C, decreasing pattern in deflection value can be observed. However, due to traffic load L_B , girder C shows smaller deflection values than under traffic load L_A .

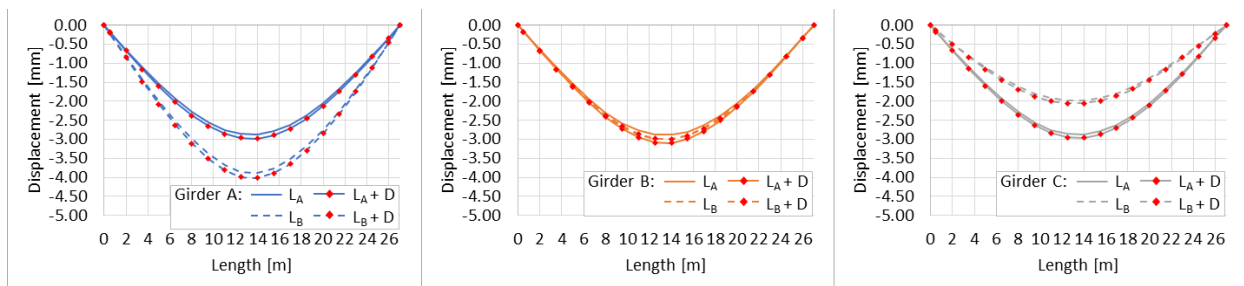


Figure 15: Bridge response under damage.

Presented in Figure 16, the Y-axis represents a change in the deformation due to traffic load L at j^{th} combination at the reference temperature. From this, the bridge response under traffic load and damage conditions for different temperature distributions results are shown. If temperature distribution yielded a smaller DAD value, such as in T1, the percent change was subtracted from the bridge response due to traffic load and damage condition at the reference temperature. On the other hand, if a larger DAD value was obtained, such as in T2, the percent change was added to the bridge response due to traffic load and damage at the reference temperature. It must be noted that the reference point for traffic load L_B deviates significantly from L_A because the reference deflections are different due to the unsymmetrical load.

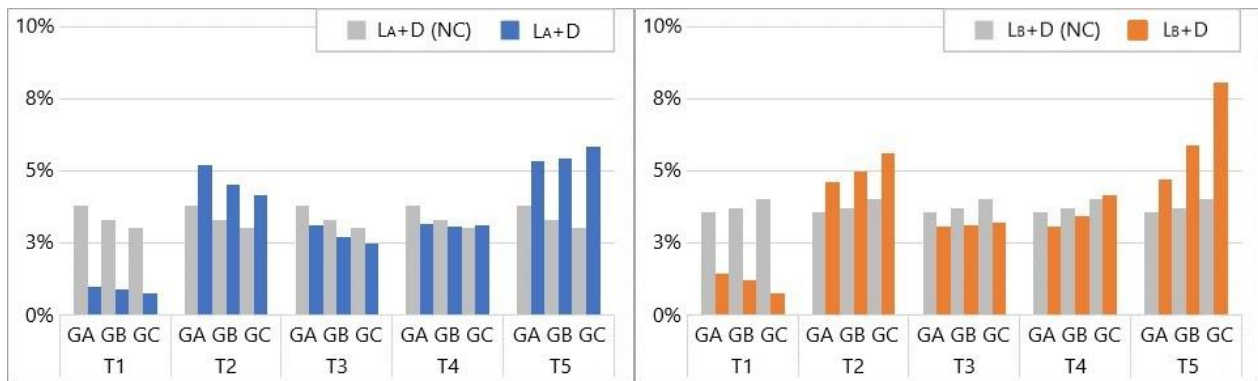


Figure 16: The DAD for different T scenarios and traffic loads when the thermal response is not characterized (grey) and characterized (coloured).

In Figure 16, when both traffic and damage are applied, the vertical displacements at T1 and T3 would decrease. The change in response at T1 is higher than at T3. At T2, the bridge response increases by a maximum of 5.21% for L_A on girder A, and 5.65% for L_B on girder C. Although the temperature distribution is at a constant 30°C, in L_A , girder A experienced a higher increase in deformation of 5.21% than girder B (4.53%), and girder C (4.15%). In L_B , girder A experienced a smaller increase 4.62% than girder B (4.97%), and girder C (5.65%). At T4, the DAD results in both positive and negative responses due to L_A but no significant changes can be observed. However, this was not the case for L_B which in comparison with L_A , changes in the responses were significant. At T5, the DAD results in the highest change in bridge response, yielding a maximum of 5.85% for L_A and 8.10% for L_B .

Table 1: The DAD due to L_A+D and $T(i)$ not characterized.

Member	Baseline	REFT		T1		T2		T3		T4		T5	
	Area (m ²)	Area (m ²)	difference	Area (m ²)	difference	Area (m ²)	difference	Area (m ²)	difference	Area (m ²)	difference	Area (m ²)	difference
Girder A	0.0487	0.0505	3.80%	0.0492	0.99%	0.0512	5.21%	0.0502	3.13%	0.0502	3.18%	0.0513	5.35%
Girder B	0.0500	0.0516	3.32%	0.0504	0.89%	0.0523	4.53%	0.0514	2.73%	0.0515	3.06%	0.0527	5.42%
Girder C	0.0487	0.0501	3.03%	0.0490	0.77%	0.0507	4.15%	0.0499	2.47%	0.0502	3.12%	0.0515	5.85%

Table 2: The DAD due to L_B+D and $T(i)$ not characterized.

Member	Baseline	REFT		T1		T2		T3		T4		T5	
	Area (m ²)	Area (m ²)	difference	Area (m ²)	difference	Area (m ²)	difference	Area (m ²)	difference	Area (m ²)	difference	Area (m ²)	difference
Girder A	0.0649	0.0672	3.57%	0.0659	1.46%	0.0679	4.62%	0.0669	3.06%	0.0669	3.10%	0.0680	4.73%
Girder B	0.0489	0.0507	3.73%	0.0495	1.24%	0.0513	4.97%	0.0504	3.12%	0.0505	3.46%	0.0517	5.88%
Girder C	0.0337	0.0350	4.02%	0.0339	0.77%	0.0356	5.65%	0.0348	3.21%	0.0351	4.15%	0.0364	8.10%

For every consecutive inspection in Figure 16, the deformation areas were found to be different for traffic load and damage when the effects of thermal response were removed. According to the results in Table 1, the deformation areas of traffic load and damage increased for girders by 0.99-0.77% in T1, 5.21-4.15% in T2, 3.13-2.47% in T3, 3.18-3.12% in T4, and lastly, 5.35-5.85% in T5. According to the results in Table 2, the deformation areas of traffic load and damage increased for girders by 1.46-0.77% in T1, 4.62-5.65% in T2, 3.06-3.21% in T3, 3.10-4.15% in T4, and lastly, 4.73-8.10% in T5.

6. Discussion

The bridge response due to unseen damage (when both traffic load and damage are applied) would decrease when the temperature is at 0°C. If the temperature is higher than the reference temperature by 10°C at T2 (30°C), the response will increase. However, when traffic load and damage are simulated during extremely hot summer days (30-50°C), the temperature would increase the bridge's response the most. Varying temperature distribution, 10-30°C results in varying deformation areas, yielding both an increase and decrease in the response.

Each traffic load was unique, therefore, L_A showed overall similar responses throughout all girders and L_B varying responses. When the thermal response is not characterized and the damage is present, in the parametric simulation, the bridge response values will change. Therefore, inaccurate conclusions about the structure's state can be made. Considering the nature of the unsymmetrical load, torsional behaviour can be also noticed. Based on the results, unsymmetrical loads (resulting in torsion) can influence the temperature effect by making it increase the magnitude of the response of the unloaded side at extreme temperatures by 8%. The higher the temperature, the larger the response of the unloaded side will be.

7. Conclusions

Bridges responses are unique and governed by temperature distribution loads which may cause major deformations larger than or equal to peak-to-peak traffic loads in the long-term. Therefore, correct characterization of the bridge thermal response is important in condition assessment. This study uses numerical replicas (in a form of a FEM) of the UT Campus bridge to show that the relationship between distributed temperature loads in the bridge response, under nominal traffic loads and damage is different. The following conclusions can be made:

- The bridge response due to traffic load and unseen damage can either increase or decrease depending on temperature distribution when its response is neglected, leading to wrong and inaccurate conclusions about the structure's state.
- Simplistic assumptions such as neglecting the thermal response are most likely to lead to errors of 8% or more under extreme temperature distributions.
- When an unsymmetrical load is present and results in torsion, the thermal response can increase as much as twice at the unloaded side.
- Changes in deformation areas can be small (~0.77%) but some could fluctuate enough to observe and potentially help study the deflection pattern.
- FEM requires comprehensive climatic data in order to account for additional cooling or heating of the surface by evaporation, precipitation, melting and freezing processes that affect the overall heat balance (Görtz, Jürgensen, Stolz, Wieprecht, & Terheiden, 2022).

During the design and inspection, it is important to account for the temperature effect because if the damage is present, the obtained bridge response would be different than when the damage is not present. The displacement values can be larger than the calculated values when assuming normal (e.g., no damage) conditions. Therefore, knowledge of the temperature effect on the bridge response when employing the parametric models can support the FEM condition assessment of bridges. However, further work is required to fully understand the complexity behind changes in the thermal response. Although no changes were observed for bridge response due to nominal traffic loads and uncharacterized thermal responses, this study investigated the effects of uncharacterized thermal response when unseen damage was present.

References

- Ansys. (2022, June 23). *What is APDL? Ansys Parametric Design Language*. Retrieved from Ansys: <https://www.ansys.com/blog/what-is-apdl>
- Ansys Learning. (2021, December 1). Overview of MAPDL — Lesson 1.
- Askegaard, V., & Mossing, P. (1998). Long term observation of RC-bridge using changes in natural frequency. *Nordic concrete research*, 20-27.
- Brenner, B. R., Sanayei, M., Bell, E. S., Rosenstrauch, P. L., Pheifer, E. J., & Marr, W. A. (n.d.). *The Influence of Temperature Changes on Bridge Structural Behavior*. Medford: Tufts University.
- Brownjohn, J. M. (2007, February 15). Structural health monitoring of civil infrastructure. *Philosophical Transactions A*, 365(1851). doi:10.1098/rsta.2006.1925
- Bud, M. A., Moldovan, I., Radu, L., Nedelcu, M., & Figueiredo, E. (2022, March 05). Reliability of probabilistic numerical data for training machine learning algorithms to detect damage in bridges. *Structural Control and Health Monitoring*, 29(7). doi:10.1002/stc.2950
- Catbas, F. N., Susoy, M., & Frangopol, D. M. (2008, September 1). Structural Health Monitoring and Reliability Estimation: Long Span Truss Bridge Application With Environmental Monitoring Data. *Engineering Structures*, 30, 2347-2359. doi:10.1016/J.ENGSTRUCT.2008.01.013
- De Battista, N., Brownjohn, J. M., Tan, H. P., & Koo, K.-Y. (2015). Measuring and modelling the thermal performance of the Tamar Suspension Bridge using a wireless sensor network. *Structure and Infrastructure Engineering*, 11(2), 176-193. doi:10.1080/15732479.2013.862727
- Doebbling, S. W., & Farrar, C. R. (1997). Using statistical analysis to enhance modal-based damage identification. *DAMAS 97* (pp. 199-210). UK: University of Sheffield.
- Erdenebat, D., Waldmann, D., Scherbaum, F., & Teferle, N. (2018, January 15). The Deformation Area Difference (DAD) method for condition assessment of reinforced structures. *Engineering Structures*, 155, 315-329. doi:10.1016/j.engstruct.2017.11.034
- European Committee for Standardization. (2003). Eurocode 1: Actions on structures - Part 1-5: General actions - Thermal actions. Brussels, Belgium.
- European Committee for Standardization. (2003). Eurocode 1: Actions on structures - Part 2: Traffic loads on bridges. Brussels, Belgium.

- Farrar, C. R., Baker, W. E., Bell, T. M., Cone, K. M., Darling, T. W., Duffey, T. A., . . . Migliori, A. (1996). *Dynamic characterization and damage detection in the I-40 bridge over the Rio Grande*. Los Alamos: U.S. Department of Energy. doi:10.2172/10158042
- Gheitasi, A., Ozbulut, O. E., Usmani, S., Alipour, M., & Harris, D. K. (2016, November 9). Experimental and analytical vibration serviceability assessment of an in-service footbridge. *Case Studies in Nondestructive Testing and Evaluation*, 6, 79-88. doi:10.1016/j.csndt.2016.11.001
- Görtz, J., Jürgensen, J., Stolz, D., Wieprecht, S., & Terheiden, K. (2022, November 15). Energy load prediction on structures and buildings-Effect of numerical model complexity on simulation of heat fluxes across the structure/environment interface. *Applied Energy*, 326. doi:10.1016/j.apenergy.2022.119981
- Goulet, J. A., Kripakaran, P., & Smith, I. F. (2015, June). Multimodel structural performance monitoring. *Journal of Structural Engineering*.
- Harish, A. (2022, October 19). *Finite Element Method – What Is It? FEM and FEA Explained*. Retrieved from SimScale: <https://www.simscale.com/blog/what-is-finite-element-method/>
- Ji, T. (2020). *Structural Design Against Deflection*. Boca Raton: CRC Press. doi:10.1201/9780429465314
- Kim, C. Y., Jung, D. S., Kim, N. S., & Yoon, J. G. (1999). Effect of vehicle mass on the measured dynamic characteristics of bridges from traffic-induced test. *IMAC XIX*, (pp. 1106-1110). Kissimmee, FL.
- Kromanis, R., & Kripakaran, P. (2014, May). Predicting thermal response of bridges using regression models derived from measurement histories. *Computers & Structures*, 136, 64-77. doi:10.1016/j.compstruc.2014.01.026
- Kromanis, R., Kripakaran, P., & Harvey, B. (2015, December). Long-term structural health monitoring of the Cleddau bridge: evaluation of quasi-static temperature effects on bearing movements. *Structure and Infrastructure Engineering*, 1342-1355. doi:10.1080/15732479.2015.1117113
- Kurloo Technology Pty Ltd. (2022, July 1). *Displacement Monitoring in Geotechnical Engineering: How It's Done and Why It's Important*. Retrieved from Kurlo: <https://www.kurloo.io/2022/07/01/displacement-monitoring-in-geotechnical-engineering-how-its-done-and-why-its-important/>

- Levings, J., & Sritharan, S. (2012, December). Effects of Cold Temperature and Strain Rate on the Stress-Strain Behavior of ASTM A706 Grade 420(60) Steel Reinforcement. *Journal of Materials in Civil Engineering*, 1441-1449. doi:10.1061/(ASCE)MT.1943-5533.0000523
- Máca, J., & Štěpánek, J. (2017). Pedestrian load models of footbridges. *MATEC Web of Conferences*. Prague: Czech Technical University in Prague. doi:10.1051/mateconf/201710700009
- Moorthy, S., & Roeder, C. W. (1992). Temperature-dependent bridge movements. *ASCE, J. Struct. Eng.*, 118, 1090-1105.
- Schroeder, D. V. (2011). *Understanding Astronomy: The Sun and the Seasons*. Retrieved from Understanding Astronomy Web site: <https://physics.weber.edu/schroeder/ua/sunandseasons.html>
- Smith, R. J. (2011). Deflection Limits in Tall Buildings—Are They Useful? *Structures Congress 2011*. Los Angeles: Arup. doi:10.1061/41171(401)45
- Sohn, H. (2006, December 13). Effects of environmental and operational variability on structural health monitoring. *Philosophical Transactions of The Royal Society A*, 539-560. doi:10.1098/rsta.2006.1935
- Tadeu, A., Romero, A., Bandeira, F., Pedro, F., Dias, S., Serra, M., . . . Galvin, P. (2022, February 15). Theoretical and experimental analysis of the quasi-static and dynamic behaviour of the world's longest suspension footbridge in 2020. *Engineering Structures*, 253. doi:10.1016/j.engstruct.2021.113830
- The Constructor. (2021, May 16). *What is Structural Health Monitoring in Civil Engineering?* Retrieved from The Constructor Web site: <https://theconstructor.org/digital-construction/structural-health-monitoring-civil-engineering/554160/>